

Urszula Rychlewska,* Agnieszka
Plutecka, Marcin Hoffmann,
Paweł Skowronek, Krystyna
Gawrońska and Jacek Gawroński

Faculty of Chemistry, Adam Mickiewicz
University, Grunwaldzka 6, 60-780 Poznań,
Poland

Correspondence e-mail: urszular@amu.edu.pl

Probing the shapes of chiral bis-(*o*-naphthalimido-benzoyl) systems using X-ray and circular dichroism methods

Received 25 July 2008

Accepted 9 December 2008

CD (circular dichroism) and X-ray investigations have been carried out in order to identify the prevalent conformations and define the forces that determine the molecular and supramolecular organization of the alkyl-bridged bichromophoric [NAB, *ortho*-(1,8-naphthalimido)benzoyl] units, each consisting of the benzoyl substituted in the *ortho* position with the 1,8-naphthalimide group. The results reveal that NAB bichromophores incorporated into the same molecule exist in a variety of conformation/helicity combinations. The molecular structures are largely stabilized by local 1,3-CH/CO dipole–dipole interactions, while the crystal packing besides dispersive H···H interactions is mostly governed by multiple C–H···O(=C) and C–H··· π interactions. The relatively small contribution of π ··· π interactions comes from a pairwise off-face stacking between naphthalimide rings or from pairwise carbonyl··· π interactions. All these types of intermolecular interactions have been summarized quantitatively by means of a Hirshfeld surface analysis.

1. Introduction

Some time ago it was demonstrated that the bichromophore consisting of a benzoyl group with a naphthalimide group substituted in the *ortho* position (the NAB bichromophore, see scheme) has the ability to act as a sensor for the chirality of aliphatic secondary alcohols (Gawroński *et al.*, 2002). These stereochemical studies, applying the Exciton Coupled Circular Dichroism (ECCD) technique, were based on the induced helicity of the NAB bichromophore and thus the induced Cotton effects within its π – π^* absorption bands. The induced helicity of the NAB bichromophore is believed to stem from the restricted rotation around the N_{imide}–C_{aryl} bond and a distortion of the NAB bichromophore from the ideal C_s-symmetry structure in its low-energy conformation owing to steric interaction. Following on from our previous studies on a monochromophoric system (Gawroński *et al.*, 2002; Plutecka *et al.*, 2007), the helical structure of NAB bichromophores observed in a crystal is an intrinsic element which is also present in isolated molecules. Combined with molecular chirality, the NAB helicity gives rise to diastereomeric pairs of molecules, which differ slightly in their energy (Plutecka *et al.*, 2007). The question of whether two such NAB units incorporated into the same molecule compete or cooperate with each other, either enhancing or hindering the overall helicity of the studied system, will be addressed in this paper. Moreover, an attempt will be made to assess the forces that influence and stabilize the overall shape and helicity of an individual NAB bichromophore, chromophores incorporated into the same molecule and chromophores self-assembled in a crystal. Herein we report the results of the X-ray analysis of

four compounds containing two NAB moieties incorporated into (*2S*)-1,2-propanediol, (*S,S*)-2,4-pentanediol, (*R,R*)-1,2-cyclohexanediol and (*R,R*)-1,2-diaminocyclohexane [(1)–(4)], and the results of the CD measurements for bis-NAB derivatives (1)–(5), and the mono-NAB derivatives of (2) and (3). The studied molecules are relatively flexible, therefore, a significant effect of both intra- and intermolecular interactions on molecular structure can be observed.

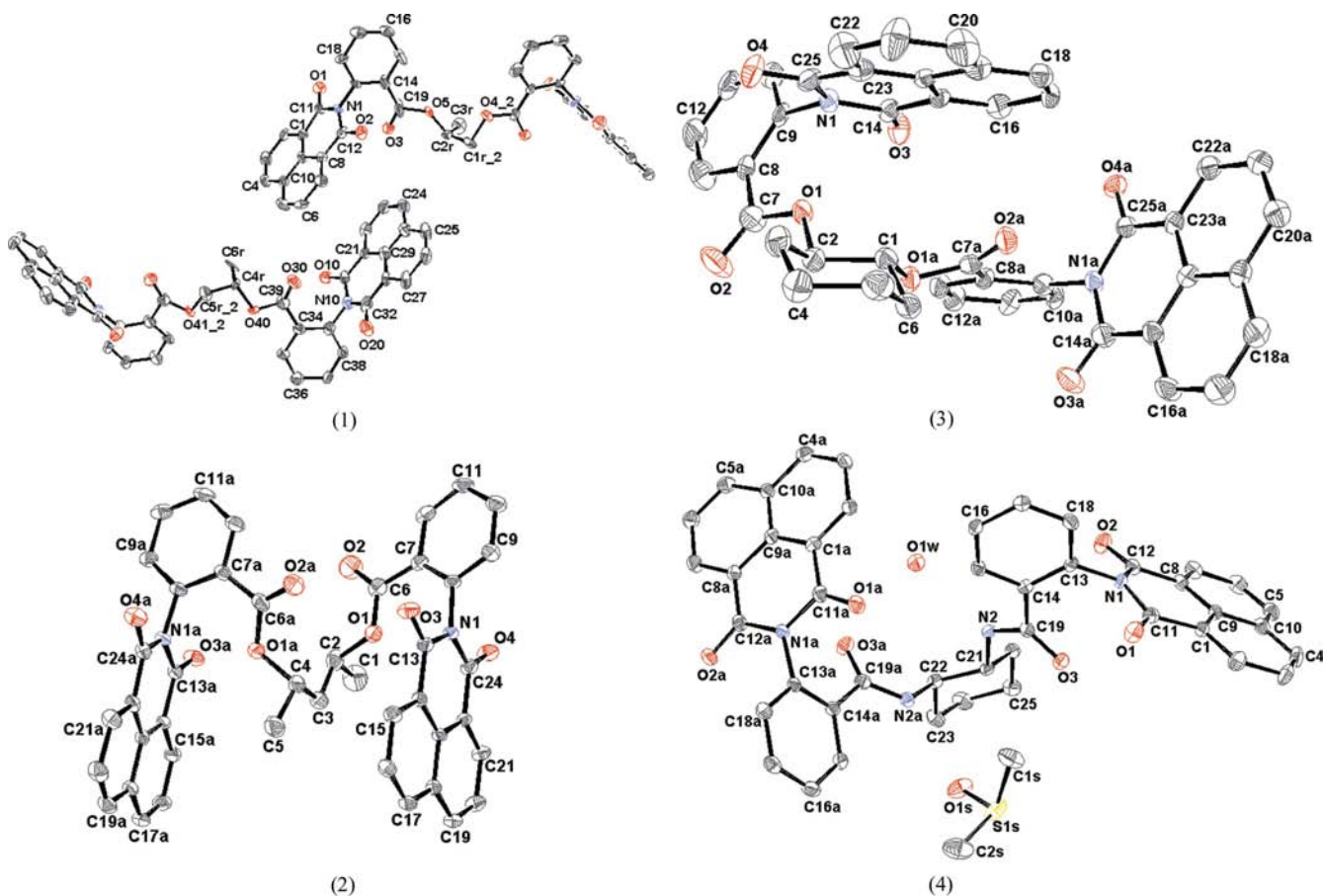
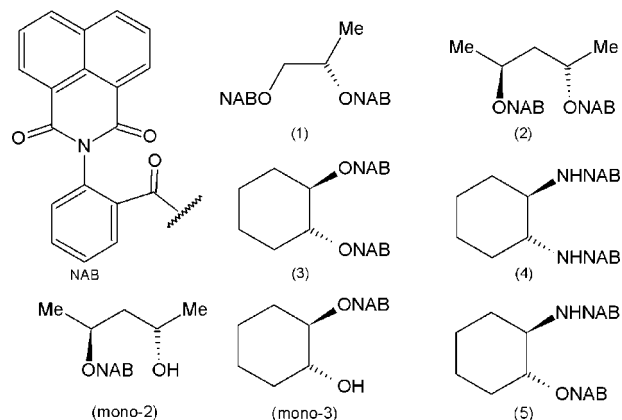


Figure 1

Displacement ellipsoid representation (at 40% probability level) of the asymmetric unit in crystals of (1), (2), (3) and (4). Atoms are numbered in sequence around the rings; atom labels not shown can be determined from those given. H atoms have been omitted for clarity. Molecules of (1) occupy the twofold symmetry site and only one of two alternative positions of the atoms constituting the diol unit is displayed. Similarly, the disorder of the DMSO molecule in a crystal of (4) is not displayed.

2. Experimental

2.1. Synthesis

Bis-NAB derivatives (1)–(5) were obtained from the corresponding commercially available diols, amino alcohol and diamine according to a previously reported procedure (Gawroński *et al.*, 2002). The corresponding mono-NAB derivatives (mono-2) and (mono-3) were obtained as more polar side products and separated by column chromatography on silica gel. All compounds were characterized spectroscopically by UV-CD, NMR and high-resolution mass spectrometry.

2.2. X-ray diffraction

The compounds investigated were difficult to crystallize and diffracted X-rays very weakly. Moreover, the crystals of (1) were twinned, making it necessary to carry out the diffraction measurements for this compound using Cu $K\alpha$ radiation. Having no access to this type of X-ray tube, we have accepted an offer by Oxford Diffraction for data collection of this compound. Reflection intensities for (1) were measured on an Xcalibur Nova diffractometer equipped with a Cu microfocus source and 165 mm Onyx CCD detector (Oxford Diffraction,

Table 1
Experimental details.

	(1)	(2)	(3)	(4)
Crystal data				
Chemical formula	C ₄₁ H ₂₆ N ₂ O ₈	C ₄₃ H ₃₀ N ₂ O ₈	C ₄₄ H ₃₀ N ₂ O ₈	C ₄₄ H ₃₂ O ₆ N ₄ ·C ₂ H ₆ OS·H ₂ O
<i>M_r</i>	674.64	702.69	714.70	808.88
Cell setting, space group	Monoclinic, <i>C2</i>	Triclinic, <i>P1</i>	Trigonal, <i>P3₂21</i>	Monoclinic, <i>C2</i>
Temperature (K)	100.0 (5)	140.0 (5)	140.0 (5)	130.0 (5)
<i>a</i> , <i>b</i> , <i>c</i> (Å)	16.9672 (9), 8.0833 (3), 25.0204 (5)	9.2897 (7), 10.0849 (7), 11.0897 (8)	11.873 (2), 11.873 (2), 43.046 (9)	22.374 (4), 9.319 (2), 20.515 (4)
α , β , γ (°)	90.00, 116.312 (3), 90.00	103.203 (6), 111.486 (7), 107.147 (6)	90.00, 90.00, 120.00	90.00, 110.14 (3), 90.00
<i>V</i> (Å ³)	3076.0 (2)	855.11 (14)	5255.1 (17)	4015.9 (16)
<i>Z</i>	4	1	6	4
<i>D_x</i> (Mg m ⁻³)	1.457	1.365	1.355	1.338
Radiation type	Cu <i>K</i> α	Mo <i>K</i> α	Mo <i>K</i> α	Mo <i>K</i> α
μ (mm ⁻¹)	0.84	0.10	0.09	0.14
Crystal form, colour	Plate, colourless	Plate, colourless	Plate, colourless	Plate, colourless
Crystal size (mm)	0.30 × 0.10 × 0.05	0.30 × 0.20 × 0.10	0.5 × 0.2 × 0.2	0.60 × 0.40 × 0.05
Data collection				
Diffractometer	Xcalibur Nova κ -geometry	Kuma KM4CCD κ -geometry	Kuma KM4CCD κ -geometry	Kuma KM4CCD κ -geometry
Data collection method	ω scans	ω scans	ω scans	ω scans
Absorption correction	Multi-scan†	None	None	Multi-scan†
<i>T_{min}</i>	0.765	–	–	0.882
<i>T_{max}</i>	0.954	–	–	0.997
No. of measured, independent and observed reflections	26 986, 2810, 2765	8911, 2994, 2388	15 932, 3556, 2230	13 581, 3769, 3166
Criterion for observed reflections	<i>I</i> > 2σ(<i>I</i>)	<i>I</i> > 2σ(<i>I</i>)	<i>I</i> > 2σ(<i>I</i>)	<i>I</i> > 2σ(<i>I</i>)
<i>R_{int}</i>	0.048	0.034	0.081	0.053
θ_{\max} (°)	65.8	25.0	25.0	25.0
Refinement				
Refinement on	<i>F</i> ²	<i>F</i> ²	<i>F</i> ²	<i>F</i> ²
<i>R</i> [<i>F</i> ² > 2σ(<i>F</i> ²)], <i>wR</i> [<i>F</i> ²], <i>S</i>	0.089, 0.247, 1.03	0.031, 0.058, 0.91	0.051, 0.126, 0.97	0.047, 0.078, 1.04
No. of reflections	2810	2994	3556	3769
No. of parameters	506	479	487	549
H-atom treatment	Constrained‡	Constrained‡	Constrained‡	Constrained‡
Weighting scheme	$w = 1/[\sigma^2(F_o^2) + (0.1555P)^2 + 10.4492P]$, where $P = (F_o^2 + 2F_c^2)/3$	$w = 1/[\sigma^2(F_o^2) + (0.030P)^2]$, where $P = (F_o^2 + 2F_c^2)/3$	$w = 1/[\sigma^2(F_o^2) + (0.0564P)^2]$, where $P = (F_o^2 + 2F_c^2)/3$	$w = 1/[\sigma^2(F_o^2) + (0.0343P)^2]$, where $P = (F_o^2 + 2F_c^2)/3$
(Δ/σ) _{max}	< 0.0001	0.001	< 0.0001	< 0.0001
$\Delta\rho_{\max}$, $\Delta\rho_{\min}$ (e Å ⁻³)	0.42, -0.41	0.16, -0.18	0.25, -0.27	0.21, -0.19
Extinction method	None	<i>SHELXL</i>	None	None
Extinction coefficient	–	0.038 (3)	–	–

Computer programs used: *CrysAlisCCD* Version 1.171.32.5 (Oxford Diffraction, 2007*a,b*), *CrysAlisCCD* Version 1.171.23 (Oxford Diffraction, 2002*a,b*), *CrysAlisRED* Version 1.171.32.5 (Oxford Diffraction, 2007*a,b*), *SHELXS97*, *SHELXL97* (Sheldrick, 2008), *XP* (Siemens, 1989), *ORTEP3* (Farrugia, 1997), *MERCURY* (Taylor & Macrae, 2001; Bruno *et al.*, 2002). † Based on symmetry-related measurements. ‡ Constrained to parent site.

2007*a,b*). In order to increase the resolution between partially overlapping reflections, the detector distance was increased to 75 mm and the scan width (on ω) was set to 0.5°. The diffraction measurements for the remaining crystals (2), (3) and (4) were carried out using the Mo radiation at the local X-ray laboratory. The intensity data were measured with a KM4CCD kappa-geometry diffractometer (Oxford Diffraction, 2002*a,b*). The temperature of the samples was controlled with an Oxford Instruments Cryosystem cold nitrogen-gas blower. The structures were solved by direct methods using *SHELXS97* and refined by least-squares techniques with *SHELXL97* (Sheldrick, 2008). The intensity data were corrected for Lp effects. An absorption correction was applied for (1) and (4) (Oxford Diffraction, 2002*a,b*, 2007*a,b*). During the refinement of structure (1), the *ROTAX* (Cooper *et al.*, 2002) procedure was used to identify the relationship between

the two domains of the twinned crystal. This was expressed by the matrix (1 0 0, 0 -1 0, -1.307 0 -1), which corresponds to a rotation of 180° about the [100] direct lattice direction. Subsequent refinement indicated that the twin fraction of the second domain was 0.216 (4). The program *WinGX* (Farrugia, 1999) was used to generate the HKLF5 file based on the twin matrix. In all the structures reported the heavy atoms (C, N, O, S) were refined anisotropically. The positions of the C–H hydrogen atoms were calculated at standardized distances of 0.96 Å and refined using a riding model, and their isotropic displacement parameters were given a value 20% higher than the isotropic equivalent for the atom to which the H atoms were attached, except for the methyl H atoms for which this value has been increased to 50%. In structure (4) the amide H atom positions were determined from difference-Fourier maps and these H atoms were also treated as riding with $U_{\text{iso}}(\text{H}) =$

Table 2

Conformation and helicity of the NAB bichromophores, described by a set of α and β torsion angles, and the various combinations of the two properties found in the molecules investigated.

	Conformer A		Conformer B		Combination of NAB conformers	Combination of NAB helicity [†]
	α (°)	β (°)	α (°)	β (°)		
(1)‡	75.8 (11)	20.4 (21)			A/A	P/P
	−72.2 (10)	−21.5 (19)			A/A	M/M
(2)			78.7 (3)	175.8 (3)	B/B	P/P
			77.1 (3)	−160.2 (3)		
(3)	73.6 (7)	21.7 (7)	−73.1 (6)	173.8 (6)	A/B	P/M
(4)	73.9 (4)	33.4 (5)			A/A	P/M
	−66.3 (4)	−26.2 (5)				

[†] Determined by the sign of angle α . [‡] The values are given for two halves of the two crystallographically independent molecules.

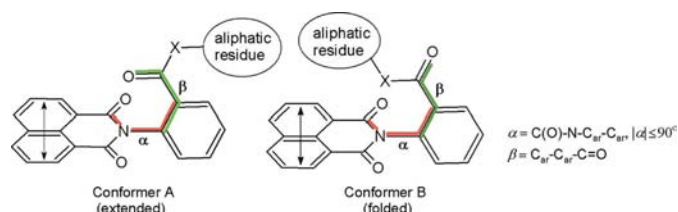
Table 3

Geometrical parameters describing the helicity of the O—C···C—O (or N—C—C—N) bond system, mutual orientation of the longitudinal naphthalene axes and distances between naphthalimide and benzoyl chromophores present in one molecule.

	(1) [†]	(2)	(3)	(4)
Configuration at the stereogenic centre	<i>S</i>	<i>S,S</i>	<i>R,R</i>	<i>R,R</i>
Torsion [in (1), (3) and (4)], and pseudotorsion [in (2)] O(N)—C···C—O(N) angle (°)	−60.0 (13)	109.7 (3)	−62.3 (5)	−57.8 (4)
Angle between the longitudinal naphthalene axes (°) [‡]	2.9	−2.7	75.1	−109.8
Naphthalimide centroid-to-centroid distance (Å)	14.430 (13)	8.105 (4)	6.845 (8)	11.985 (5)
Phenyl centroid-to-centroid distance (Å)	14.708 (16)	7.359 (4)	7.035 (9)	7.531 (5)
	7.927 (19)	8.098 (18)		

[†] Two independent molecules. [‡] Calculated as a pseudo-torsion angle between the longitudinal axes of the naphthalene rings.

1.2 $U_{\text{iso}}(\text{N})$. In the structure of (1) one could clearly locate the disordered regions of the diol units. This disorder was imposed by the crystal symmetry, as the molecules lacking C_2 symmetry occupied the twofold symmetry site in the unit cell. Therefore, atoms labeled C1R–C6R, and atoms O4, O5, O40 and O41 were given an occupancy factor of 0.5. Moreover, crystals of (1) displayed severe pseudosymmetry (pseudo-inversion centre), but the possibility of the presence of this symmetry element was rejected on the grounds of the known homochirality (enantiopurity) of all the crystals investigated. Also in the crystal structure of (4) the DMSO atoms (S1S, C1S and O1S) were found to be disordered over two alternative orientations. Two positions were defined for each of these

**Figure 2**

Two possible conformations of NAB units ($X = \text{O}, \text{NH}$). Arrows mark the transition moments oriented along the longitudinal axes of the naphthalene rings.

atoms, and refinement of the site-occupation factor yielded a value of 0.880 (7) for the major component (atoms S1S, O1S and C1S). The absolute structure of the crystals was assumed from the known absolute configuration of the diols and diamines used in syntheses and no attempt was made to refine the Flack parameter. The relevant crystal data collection and refinement parameters are listed in Table 1.¹

2.3. CD measurements

CD spectra were measured with a Jasco J-910 spectropolarimeter in acetonitrile-dioxane (9:1) solutions at concentrations of $10^{-4} \text{ mol l}^{-1}$.

3. Results and discussion

3.1. Molecular structures

Perspective views of the investigated molecules are shown in Fig. 1. Geometrical parameters describing the conformation and helicity of the single NAB moieties, as observed in the investigated crystals, are listed in Table 2. Table 3 lists the geometrical parameters that describe the mutual orientation of the two NAB bichromophores

present in each of the investigated molecules.

The molecules investigated can be treated as consisting of two parts: either a linear or cyclic aliphatic core and the *ortho*-(1,8-naphthalimido)benzoyl (NAB) moieties, in all but one case attached (*via* O or N atoms) to two stereogenic centres. The NAB units can exist in two different conformations, extended and folded (designated as A and B, respectively), differing in the degree of rotation of the carbonyl group in the benzoyl moiety with respect to the naphthalimide ring (Fig. 2). In the A conformation the carbonyl group is placed above the naphthalimide unit, while in the B conformation it is placed away from the naphthalimide unit, which is now exposed to the alkyl residues. The overall conformation of the NAB moiety can be described by a set of two torsion angles α and β , defined in Fig. 2 (Gawroński *et al.*, 2002). The α angle determines the relative orientation of the phenyl and naphthalimide rings, while β describes the mutual orientation and degree of coplanarity of the phenyl and the carbonyl groups forming the benzoate/benzamide substituent. Inspection of the Cambridge Structural Database (CSD, Version 5.28; Allen, 2002) reveals that among 74 aryl-substituted naphthalene-1,8-dicarboximides the absolute value of the α angle varies from

¹ Supplementary data for this paper are available from the IUCr electronic archives (Reference: SO5018). Services for accessing these data are described at the back of the journal.

55.5 to 90.0°. When different from 90°, the sign of the α angle determines the helicity of the NAB bichromophore. Usually the β angle should adopt either a value close to 0° (the *A* conformer) or to 180° (the *B* conformer). Values significantly different from 0 and 180° lead towards the question as to whether their sign is coupled with the sign of the α angle.

The molecules of (1) are situated on the twofold axis in spite of the fact that they lack the C_2 symmetry. This implies a disorder of both the aliphatic chain and the O atoms directly attached to it. The asymmetric unit comprises two halves of the two crystallographically independent molecules. As to the individual NAB moieties, inspection of Table 2 reveals that the main source of the NAB helicity is the fact that the mutual orientation of the naphthalimide and phenyl rings is not strictly perpendicular. As required by the twofold symmetry, each of the two independent molecules of (1) contains NAB units of the same helicity, but in one of them the helicity is *P/P* (positive values of α) while in the other it is *M/M* (negative values of α). The values of the β angle indicate that in both

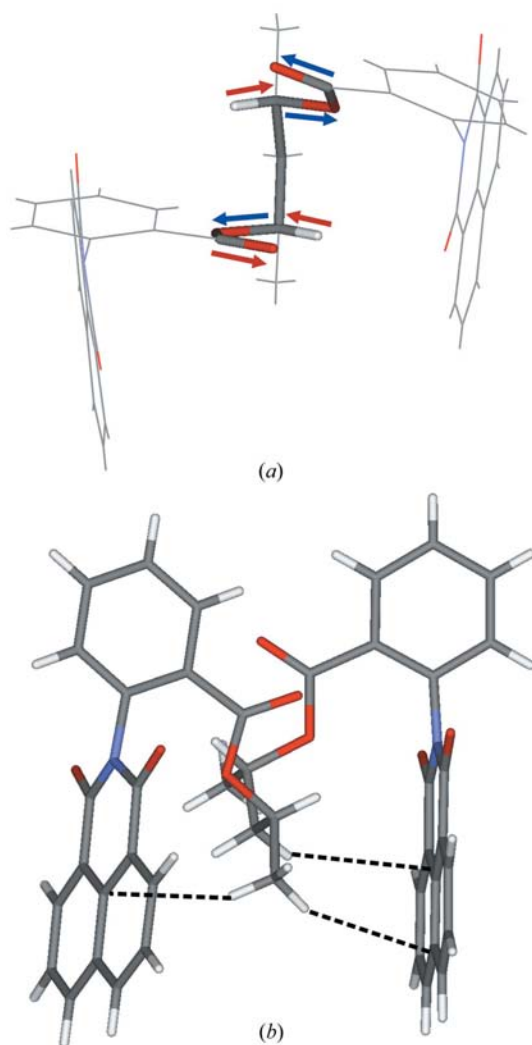


Figure 3
Multiple intramolecular interactions in (2). (a) Interactions between 1,3-CO/CH antiparallel local dipoles; (b) C-H(aliphatic)···π(aromatic) interactions.

Table 4

Geometrical parameters, as defined by Allen *et al.* (1998), describing intramolecular C—H/C=O 1,3-dipole–dipole interactions stabilizing the helicity of the NAB bichromophores.

Compound	d_1 (Å)	d_2 (Å)	Angle between C—O/C—H dipoles (°)
(1)			
C19=O3/H2RA—C2R	2.46	2.554 (17)	161
C19A ⁱ =O3A ⁱ /H1A ⁱ —C1R ⁱ	2.38	2.502 (16)	169
C39=O30/H4—C4R	2.29	2.344 (14)	162
C39A ⁱⁱ =O30A ⁱⁱ /H5A ⁱⁱ —C5R ⁱⁱ	2.37	2.506 (20)	172
(2)			
C6A=O2A/H4—C4	2.32	2.418 (4)	179
C6=O2/H2—C2	2.37	2.398 (4)	151
C4—O1A/H2—C2	2.55	2.566 (4)	180
C2—O1/H4—C4	2.66	2.566 (4)	180
(3)			
C7=O2/H2—C2	2.45	2.399 (9)	151
(4)			
C19A=O3A/H22—C22	2.39	2.457 (5)	173
C19=O3/H2—C21	2.45	2.452 (5)	154

Symmetry codes: (i) $1 - x, y, 1 - z$; (ii) $1 - x, y, -z$.

Table 5

Intramolecular C—H··· π interactions arising from the folded *B* conformation of the NAB bichromophore in (2) and (3).

C_{nph} – centre of the naphthalimide unit.

Molecule	H···A (Å)	D···A (Å)	D—H···A (°)
(2)			
C5—H5B··· C_{nph}	3.01	3.833 (4)	145
C5—H5C···C16	3.05	3.805 (4)	137
C3—H3A··· C_{nph}	3.14	3.939 (4)	142
(3)			
C1—H1··· C_{nph}	2.92	3.847 (6)	161
C3—H3B···C22	3.09	4.040 (7)	169

molecules of (1) the NAB bichromophores adopt the extended *A* conformation and that the benzoyl groups are not strictly planar. We also note that the α and β angles are paired in sign (Table 2).

Unlike in (1), where the two NAB bichromophores are situated in vicinal positions, in (2) they are separated by the methylene bridge. The bichromophores are attached to the five-carbon chain at the 2,4-positions and the chain adopts the extended *T* conformation, the corresponding torsion angles being -179.7 (3) and 173.2 (2)°. The entire chain is flanked by the two NAB units which create favourable conditions for the intramolecular C—H(aliphatic)··· π (aromatic) interactions (see below). Inspection of Table 2 reveals that both bichromophores in (2) display the same helicity and adopt the same folded *B* conformation. Unlike in (1) and in the remaining two derivatives (3) and (4), where the mutual arrangement of the two naphthalimide fragments is roughly perpendicular [the angles between the naphthalimide rings amount to 85.0 (1), 80.6 (1) and 61.5 (1)°, respectively], it is nearly parallel in (2), the corresponding value being 17.4 (1)°.

Table 6

Intermolecular hydrogen-bond parameters.

 C_{ph} – centre of gravity of the phenyl ring, (ar) – C atom constituting the aromatic ring.

	H...A (Å)	D...A (Å)	D–H...A (°)
(1)			
C16–H16...O1(=C) ⁱ	2.61	3.198 (11)	122
C16–H16...O3(=C) ⁱⁱ	2.66	3.329 (11)	130
C3–H3...O2(=C) ⁱⁱⁱ	2.28	3.145 (11)	154
C26–H26...O10(=C) ^{iv}	2.33	3.193 (10)	153
C36–H36...O20(=C) ^v	2.57	3.193 (11)	125
C36–H36...O30(=C) ^{vi}	2.81	3.406 (14)	123
(2)			
C16–H16...O4(=C) ^{vii}	2.37	3.112 (3)	133
C16A–H16A...O3(=C) ^{viii}	2.66	3.231 (3)	119
C21–H21...O2A(=C) ⁱⁱ	2.71	3.473 (3)	137
C20A–H20A...O3A(=C) ^{vii}	2.52	3.202 (3)	128
C10–H10...O4A(=C) ^{ix}	2.71	3.231 (3)	129
(3)			
C6–H6B...O3A(=C) ^x	2.42	3.059 (5)	115
C4–H4A...O3A(=C) ^x	2.79	3.364 (7)	140
C22–H22...C24A(ar) ⁱⁱ	2.67	3.451 (8)	139
C21–H21...C19A(ar) ⁱⁱ	2.87	3.565 (9)	130
C20–H20...C22A(ar) ^{xi}	2.70	3.632 (8)	164
(4)			
N2–H2N...O1W	1.99	2.925 (4)	158
N2A–H2NA...O1S	2.00	2.854 (6)	146
N2A–H2NA...O2S	1.80	2.696 (34)	153
O1W–H1W...O3A(=C)	2.15	3.042 (4)	151
O1W–H2W...O1(=C) ⁱⁱ	1.99	2.968 (4)	173
C3–H3...O2(=C) ^{vi}	2.39	3.282 (5)	154
C17A–H17A...O2A(=C) ^{xiii}	2.58	3.442 (5)	149
C6–H6...O3(=C) ^{xiii}	2.38	3.232 (7)	148
C15A–H15A...O1S	2.57	3.384 (7)	142
C15A–H15A...O2S	2.57	3.393 (39)	133
C4A–H4A...C ⁱⁱ _{ph}	2.67	3.517 (4)	147
C18–H18...C ⁱⁱⁱ _{ph}	2.85	3.755 (4)	157
C6A–H6A...C ⁱⁱ _{ph}	2.80	3.577 (4)	138
C5A–H5A...C15(ar) ⁱⁱ	2.80	3.572 (5)	138

Symmetry codes: (i) $\frac{3}{2} - x, \frac{1}{2} + y, 1 - z$; (ii) $x, 1 + y, z$; (iii) $\frac{1}{2} + x, -\frac{1}{2} + y, z$; (iv) $-\frac{1}{2} + x, \frac{1}{2} + y, z$; (v) $\frac{1}{2} - x, -\frac{1}{2} + y, -z$; (vi) $x, -1 + y, z$; (vii) $x + 1, y, z$; (viii) $x, y, z - 1$; (ix) $x, 1 + y, 1 + z$; (x) $y, x, -z$; (xi) $x - y, 1 - y, \frac{1}{3} - z$; (xii) $\frac{1}{2} - x, -\frac{1}{2} + y, -z + 1$; (xiii) $-x + 1, y, -z$.

Molecules of (3) contain two NAB bichromophores attached to the rigid cyclohexane ring in the 1,2 position and in a (–) synclinal orientation (Table 3); the ring adopts a chair conformation. Table 2 shows that the two NAB units belonging to one molecule differ in both conformation and helicity. The *A* conformer displays *P*, while the *B* conformer *M* helicity.

Replacement of the ester group in (3) by the N–H amide in (4) introduces large changes at both the molecular and supramolecular level. Compound (4) crystallizes with water and DMSO solvents in a 1:1:1 ratio. Table 2 shows that molecules in the crystal contain both NAB bichromophores in an extended *A* conformation, but the two *A* conformers present in one molecule display the opposite helicity.

The common characteristics of all the NAB units (Table 2) are that the two chromophores constituting the unit are arranged in a helical manner and the angles between the naphthalimide dipole vector (defined as running from the

centre of the fused aromatic rings through the N atom) and the benzoyl group dipole vector (defined as running from the centre of the phenyl group through the C atom of the C=O group) adopt values which lie in the narrow range 49.4 (2)–64.9 (3)°. In the majority of cases, the benzoyl group shows significant nonplanarity (described by the values of the β angle listed in Table 2), the effect being more pronounced in those NAB bichromophores that adopt the extended *A* conformation. As far as the mutual orientation of the two NAB units is concerned the distance between the centres of the benzene rings in the benzoyl groups is fairly constant in all the molecules investigated and ranges from 7.035 (9) to 8.098 (18) Å, while the angle between the two benzene rings varies significantly, differentiating between derivatives attached to the chain or ring aliphatic core [average values 20.0 (4) versus 73.2 (1)°, respectively].

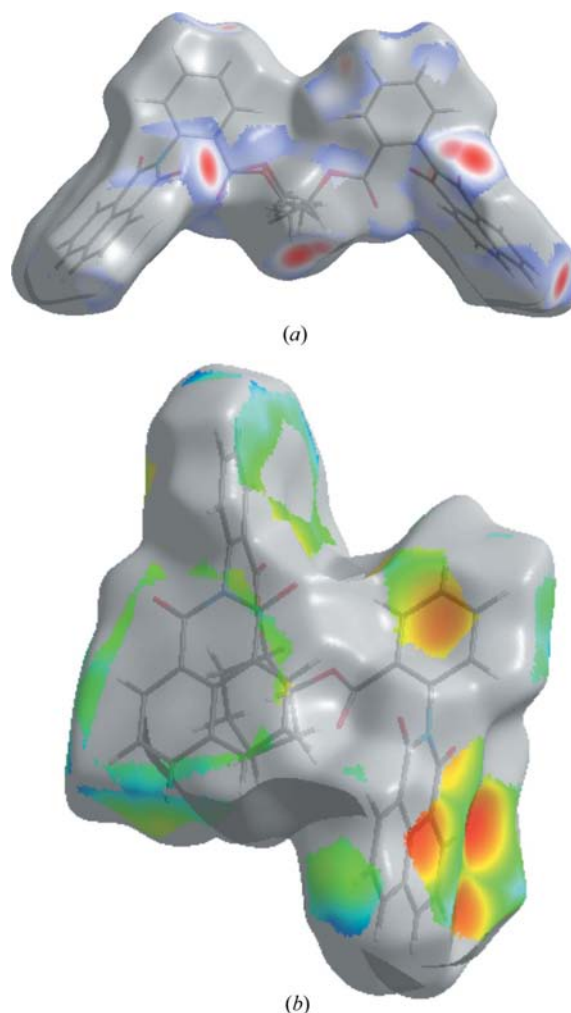


Figure 4
(a) Semi-transparent d_{norm} surface of (1). Areas involved in C–H...O(=C) hydrogen bonds appear as slight holes coloured in red; (b) d_e surface for (3). Parts of the naphthalimide ring coloured in red reveal close contacts between molecules involved in C–H... π intermolecular interactions.

3.2. Factors stabilizing the molecular conformation

With regard to the factors that could stabilize the conformation of the investigated molecules we have considered the possibility of attractive interactions between the CO dipoles belonging to the benzoyl moiety and the CH dipoles situated on the C atom to which the NAB bichromophore containing this benzoyl moiety is attached. The parameters describing this type of interaction are listed in Table 4. As can be seen from this table, the antiparallel arrangement of the C—H and C=O dipoles situated in the 1,3-position with respect to each other is observed in all the molecules investigated. The arrangement of these dipoles in molecule (2) is shown in Fig. 3(a). We have already signaled the crucial role of 1,3-CH/CO dipole–dipole interactions in stabilizing the molecular conformation of tartaric acid derivatives and salts (Gawroński *et al.*, 2005). Furthermore, the NAB units in the *B* conformation are involved in intramolecular C—H(aliphatic)·· π (aromatic) interactions which together with 1,3-CH/CO local dipole–dipole interactions might stabilize the overall conformation of molecules (2) and (3), *i.e.* in molecules containing at least one NAB unit in the folded *B* conformation.

Parameters describing intramolecular alkyl/aryl interactions are provided in Table 5. Molecule (2) is particularly rich in both kinds of interactions and contains both bichromophores in the *B* conformation. Figs. 3(a) and (b) illustrate the multiplication of C—H/C=O dipole/dipole and C—H(aliphatic)·· π (aromatic) interactions in (2).

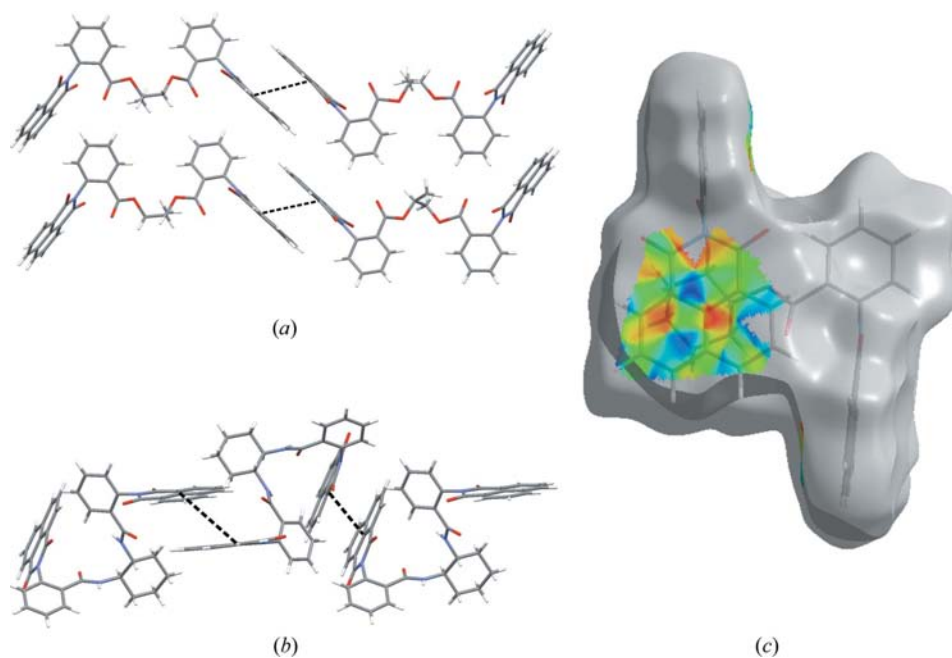


Figure 5

(a), (b) Pairwise stacking interactions in crystals of (1) and (4) involving both naphthalimide rings present in a molecule, (c) semi-transparent surface of (3) showing the area engaged in pairwise stacking interactions. At the far right of (c) the indentations on the surface reflect intermolecular C—H·· π interactions shown in Fig. 4(b), which involve the naphthalimide ring not engaged in stacking.

3.3. Intermolecular interactions in crystals

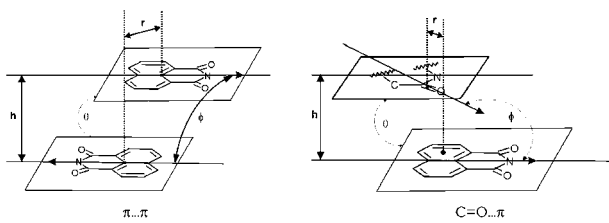
We have explored the complex mix of intermolecular interactions by applying the geometrical criteria provided by Desiraju & Steiner (1999), and by using a Hirshfeld surface analysis (McKinnon *et al.*, 2004, 2007; Spackman & Jayatilaka, 2009), as implemented in the *CrystalExplorer* program (Wolff *et al.*, 2007). Using this program we were able to quantify the amount of molecular surface involved in various interaction types. It appeared that in the investigated crystal structures the H··H dispersion interactions involve from 38% [in (1)] to 47% [in (3)] of the molecular surface area. Second in rank are weak hydrogen bonds, nearly equally distributed between C—H··O(=C) and C—H·· π types, each comprising from 22 to 27% of the surface area. Patches of the molecular surfaces involved in these interactions in molecules (1) and (3) are displayed in Fig. 4. Geometrical parameters describing these types of intermolecular interactions are listed in Table 6.

Dispersion and weak hydrogen-bond intermolecular interactions are nearly equally distributed in all the investigated crystal structures, so they might be expected to influence the observed molecular conformations to nearly the same extent. Having in mind the conformational variety of the investigated bichromophores we continued to search for other forces that might influence and stabilize the overall shape and helicity of an individual NAB bichromophore. We have found that the off-face pairwise π ·· π stacking between two naphthalimide moieties is observed in crystals of (1), (3) and (4), but not in (2). The surface area involved in such interactions is small and

varies from 5 [in (4)] to 7% [in (1)]: in (1) and (4) it engages both naphthalimide rings present in a molecule, while in (3), where it covers 6% of the molecular surface, it involves only one of them. Fig. 5 illustrates the various ways this face-to-face stacking is realised in crystals of (1) and (4), and a patch on the Hirshfeld surface of the molecule of (3) involved in these interactions. Parameters describing intermolecular stacking interactions are listed in Table 7. In (1) the interacting naphthalimide rings are oriented antiparallel, as shown in Fig. 5(a), and the stacking involves NAB units of opposite helicity. Somewhat similar but columnar-type stacking has been previously observed in the crystal structure of the compound containing only one NAB unit [(*S*)-2 butyl-*N*-(1,8-naphthaloyl)-2-aminobenzoate; Plutecka *et al.*, 2007]. It also involved naphthalimide rings oriented antiparallel and belonging to NAB bichromo-

Table 7

 Parameters describing the various types of $\pi \cdots \pi$ intermolecular interactions.



	h (Å)	θ (°)	r (Å)	φ (°)
$\pi_{\text{nphth}} \cdots \pi_{\text{nphth}}$				
(1) C1 \div C12 \cdots C21 \div C32 I	3.406 (9)	0.6 (3)	1.58 (1)	179.8 (3)
(3) C14 \div C25 \cdots C14 II \div C25 II	3.514 (5)	6.5 (1)	0.57 (1)	104.6 (2)
(4) C1 \div C12 \cdots C1 III \div C12 III	3.514 (4)	7.8 (1)	2.72 (1)	152.7 (2)
C1A \div C12A \cdots C1A IV \div C12A IV	3.343 (4)	6.1 (1)	1.95 (1)	132.4 (2)
$\text{C}=\text{O} \cdots \pi_{\text{nphth}}$				
(2) C24 \equiv O4 \cdots C18A V \div C23A V	3.717 (4)	17.1 (1)	0.25 (1)	56.2 (2)
C13A \equiv O3A \cdots C14 VI \div C18 VI /C23 VI	3.326 (4)	14.7 (1)	0.97 (1)	57.6 (2)

 Symmetry codes: (i) $\frac{1}{2} + x, \frac{1}{2} + y, z$; (ii) $-x - y + 1, -y + 2, \frac{1}{3} - z$; (iii) $-x + 1, y, -z$; (iv) $-x + 1, y, -z + 1$; (v) $x, y + 1, z + 1$; (vi) $x - 1, y - 1, z - 1$.

phores of opposite helicity. Unlike in (1), pairwise stacking interactions between naphthalimide rings in (4) involve NAB units of the same helicity, as they occur between symmetrically equivalent rings (Fig. 5*b*). Pairs of interacting naphthalimide fragments are twisted with respect to each other at angles of 132.4 (2) and 152.7 (2)° and display a different degree of overlap (Table 7). In (3), where only one of the two naphthalimide fragments is engaged in stacking, the stacking necessarily involves two NAB units of the same helicity. The two interacting rings are twisted with respect to each other by 104.6 (2)° and the degree of their overlap is the highest among the three crystal structures (Table 7).

Compound (4) crystallizes with solvent DMSO and water molecules that are situated in voids formed by four neighboring molecules. As expected, all three component molecules are involved in strong hydrogen bonding. The hydrogen-bonding parameters are provided in Table 6.

The molecules of (2) which contain the two NAB units in the *B* conformation pack differently from the others. Instead of the expected face-stacking interactions, we observe a pattern in which the carbonyl groups place themselves close to, and roughly parallel to, the face of the aromatic rings which constitute the naphthalimide fragment (Fig. 6, Table 7). This might be an indication of the presence of intermolecular $\text{C}=\text{O} \cdots \pi$ (aromatic) interactions, possibly due to the electron-deficient properties of the naphthalimide unit. Experimental evidence for carbonyl $\cdots\pi$ -electron cloud interactions has been provided by García-Bàez *et al.* (2003), Hoffmann *et al.* (2005), Yang *et al.* (2005), Gautrot *et al.* (2006) and Wan *et al.* (2008).

The percentage of the molecular surface involved in such interactions in (2), although small (5%), is the largest in the series studied at the expense of $\pi \cdots \pi$ interactions which in this case involve less than 3% of the molecular surface.

3.4. CD study

CD spectroscopy is a powerful technique for studying the stereostructures of organic molecules in solution. Previously we have shown (Gawroński *et al.*, 2002) that the NAB derivatives of aliphatic alcohols can be used as sensitive and practical chromophoric derivatives for the determination of their absolute configuration. The method is based on the induction of the preferred helicity of the NAB π -electron system owing to the differentiating steric effect exerted by the two substituents at the chiral C atom of the secondary alcohol molecule. The *P* helicity of the NAB bichromophore leads to a negative exciton Cotton effect in the range 240–210 nm, whereas the *M* helical NAB chromophore produces a positive exciton Cotton effect. A similar mechanism for the induction of the exciton Cotton effect was reported for *N*-(1,8-naphthaloyl)-3-amino-2-naphthaloyl (NAN) derivatives of chiral amines (Gawroński & Grajewski, 2004).

In the present study we aimed to show that CD spectroscopy provides information on the conformation of NAB bichromophores in molecules (1)–(5) in solution and that this information can be compared with the data obtained by X-ray diffraction of crystals of (1)–(4). In order to correctly analyze the origin of the CD spectra of bis-NAB molecules, we began with a comparison of the CD spectra of mono- and bis-NAB derivatives, *i.e.* (mono-2), (2), (mono-3) and (3) (Table 8).

The (mono-2) derivative shows a positive exciton Cotton effect ($A = 16.8$), in accordance with the model reported earlier (Gawroński *et al.*, 2002) for alkyl methyl alcohols of *S* configuration. Furthermore, the bis-NAB derivative (2) also shows a positive exciton Cotton effect (amplitude $A = 39.8$), only slightly more than twice the value of A for (mono-2). This means that the two NAB bichromophores in (2) are independent to a large extent, both conformationally and spectroscopically, *i.e.* there is little exciton interaction between the two NAB bichromophores in (2), a derivative of a 1,3-diol system. The CD model refers to an extended NAB conformation, whereas the X-ray study revealed folded conformations for both NAB bichromophores in the crystal. Note that in the crystal structure the transition moments oriented along the longitudinal axes of the two naphthalene rings of NABs are nearly parallel to each other (Table 3). This would suggest that for such a structure the exciton interaction to the CD spectrum of (2) would be small.

A small negative exciton Cotton effect ($A = -7.5$) for (mono-3) and a strong positive exciton Cotton effect ($A = 90.4$) for (3) indicate that the origin of the CD spectrum of the latter compound is due to the exciton interaction between the two NAB bichromophores. Indeed, a strong positive exciton Cotton effect of (3) can be correlated with a positive angle (75.1°) between the transition moments oriented along the longitudinal axes of the naphthalene rings and a short distance

Table 8

CD data for the investigated NAB derivatives in acetonitrile–dioxane (9:1) solution.

Compound	Long-wavelength Cotton effect		Exciton Cotton effect		Exciton amplitude (A), $\Delta\epsilon$
	$\Delta\epsilon$ (nm)	$\Delta\epsilon$ (nm)	$\Delta\epsilon$ (nm)	$\Delta\epsilon$ (nm)	
(1)	4.1 (347)	–31.4 (238)	23.1 (227)	–54.5	
(2)	0.7 (343)	28.2 (243)	–11.6 (210)	39.8	
Mono-(2)	<i>ca</i> 0	12.5 (240)	–4.3 (222)	16.8	
(3)	–9.7 (348)	62.5 (239)	–27.9 (225)	90.4	
Mono-(3)	<i>ca</i> 0	–6.1 (243)	1.4 (224)	–7.5	
(4)	–7.3 (350)	63.3 (234)	–25.1 (212)	88.4	
(5)	–7.2 (349)	47.4 (237)	–19.4 (214)	66.8	

between the NAB bichromophores in the crystal (Table 3). Thus, in the case of (3) the crystal structure correlates well with the CD data collected for this compound in solution. For (mono-3) a negative exciton Cotton effect requires a dominant *P* helicity of the NAB bichromophore in an extended (*A*) conformation, in agreement with the model presented earlier (Gawroński *et al.*, 2002).

The Cotton effects of the bis-NAB derivative (1) are of opposite sign to those of (3), with lower values apparently due to the flexible nature of the parent acyclic diol. The preferred conformation of (1) in solution therefore should be pseudoenantiomeric to (3). Acyclic terminal 1,2-diols and their ester derivatives are known to exist as mixtures of *anti* and *syn* conformers, with the former dominating (Gawroński & Gawrońska, 1990). Indeed, in a conformer of (1) with an *anti* arrangement of the C–C–C–O bond system, the helicity of the O–C–C–O bonds is *P*. However, in the two independent molecules of (1) in the crystal the C–C–C–O chain is in a bent (+)-*syn* conformation [the corresponding torsion angles in the two independent molecules being 65.7 (17) and 60.0 (19)°] and the O–C–C–O bond system is *M*-helical (the corresponding torsion angles being –60.0 (13) and –57.3 (20)°), as in (3) where the O–C–C–O torsion angle amounts to –62.3 (5)° (Table 3). In addition, the distance between the naphthalimide rings in the crystal structure of (1) is unusually long [average value 14.6 (1) Å, Table 3]. Most probably the two naphthalimide rings were directed outwards to enable the participation of both of them in face-stacking interactions. These data lead to the conclusion that the conformations of (1) in the crystal and in solution are quite different.

For the bis-NAB derivative (4) the sign and the magnitude of the exciton Cotton effects are very similar to those of (3). On the other hand, the crystal structures of (3) and (4) differ, *i.e.* the extended conformation of both NAB bichromophores in (4) contrasts with the extended/folded combination present in the crystal of (3). As a consequence, the distance between the NAB bichromophores in (4) is much longer [11.985 (5) Å] compared with 6.845 (8) Å in the case of (3). Here again the longer distance between the two naphthalimide rings most probably results from the involvement of both of them in intermolecular face-stacking interactions. We therefore conclude that unlike in the crystal where the molecular conformation of (4) is influenced by the DMSO and water

solvent molecules, the preferred conformations of (3) and (4) in solution are similar. We also observe that CD data for the bis-NAB derivative of *trans*-2-aminocyclohexanol (5) point to a coincidence of conformational preferences of the NAB bichromophores in (3)–(5) in solution.

4. Conclusions

In the investigated group of NAB derivatives of chiral diols and diamines the pairs of NAB units appear in different combinations of helicity (*P*, *M*) and conformation (extended, folded) in the crystal. This indicates that changes in molecular conformation require little energy and can be introduced by relatively weak forces. The opposite helicity seems to occur whenever the two NAB units are introduced to the rigid aliphatic core in the vicinal positions. The investigated molecules form numerous C–H···O(=C) and C–H··· π hydrogen bonds and these involve a substantial fraction of their molecular surface area. Also prevalent are intermolecular interactions that involve electron-deficient naphthalimide rings, namely the pairwise face-to-face π -stacking and the carbonyl··· π interactions. On the other hand, solution studies by CD spectra show that for mono-NAB derivatives the extended conformation *A* prevails, as previously postulated. For bis-NAB derivatives only in the case of a derivative of 1,3-diol a model of two independent NAB bichromophores in an extended conformation appears valid, whereas bis-NAB derivatives of 1,2-diols show a more complicated conformational profile. Therefore, in contrast to an X-ray diffraction study, no single preferred structure can be postulated from an analysis of the CD spectra of such derivatives in solution.

The authors (UR and AP) wish to thank Zoltan Gal and Oxford Diffraction for performing the data collection for the severely twinned crystals of (1), and Professor Mark A. Spackman for providing access to the *CrystalExplorer* program.

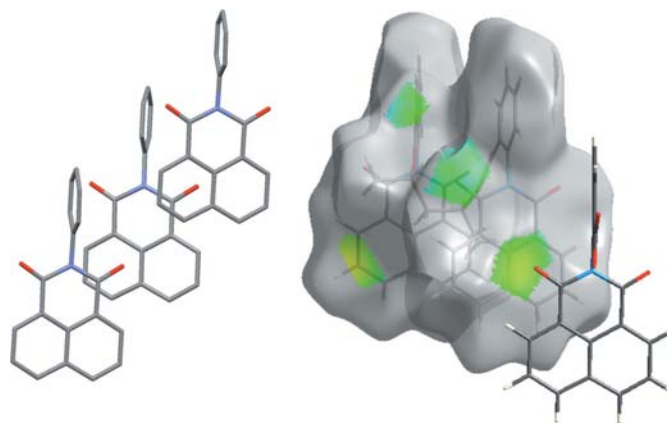


Figure 6
Carbonyl··· π (arene) interactions in the crystal structure of (2): view perpendicular to the best plane of one of the naphthalimide rings. H atoms were omitted for clarity.

References

- Allen, F. H. (2002). *Acta Cryst.* **B58**, 380–388.
- Allen, F. H., Baalham, C. A., Lommerse, J. P. M. & Raithby, P. R. (1998). *Acta Cryst.* **B54**, 320–329.
- Bruno, I. J., Cole, J. C., Edgington, P. R., Kessler, M., Macrae, C. F., McCabe, P., Pearson, J. & Taylor, R. (2002). *Acta Cryst.* **B58**, 389–397.
- Cooper, R. I., Gould, R. O., Parsons, S. & Watkin, D. J. (2002). *J. Appl. Cryst.* **35**, 168–174.
- Desiraju, G. R. & Steiner, T. (1999). *The Weak Hydrogen Bond*, p. 44. New York: Oxford University Press.
- Farrugia, L. J. (1997). *J. Appl. Cryst.* **30**, 565.
- Farrugia, L. J. (1999). *J. Appl. Cryst.* **32**, 837–838.
- García-Bàez, E. V., Martínez-Martínez, F. J., Höpfl, H. & Padilla-Martínez, I. I. (2003). *Cryst. Growth Des.* **3**, 35–45.
- Gautrot, J. E., Hodge, P., Cupertinob, D. & Helliwell, M. (2006). *New J. Chem.* **30**, 1801–1807.
- Gawroński, J., Długokińska, A., Grajewski, J., Plutecka, A. & Rychlewska, U. (2005). *Chirality*, **17**, 388–395.
- Gawroński, J. & Gawrońska, K. (1990). *Carbohydr. Res.* **206**, 141–151.
- Gawroński, J. & Grajewski, J. (2004). *Tetrahedron Asymmetry*, **15**, 1527–1530.
- Gawroński, J., Kwit, M. & Gawrońska, K. (2002). *Org. Lett.* **4**, 4185–4188.
- Hoffmann, M., Plutecka, A., Rychlewska, U., Kucybała, Z., Pączkowski, J. & Pyszka, I. (2005). *J. Phys. Chem. A*, **109**, 4568–4574.
- McKinnon, J. J., Jayatilaka, D. & Spackman, M. A. (2007). *Chem. Commun.* pp. 3814–3816.
- McKinnon, J. J., Spackman, M. A. & Mitchell, A. S. (2004). *Acta Cryst.* **B60**, 627–668.
- Oxford Diffraction (2002a). *CrysAlis CCD*. Oxford Diffraction, England.
- Oxford Diffraction (2002b). *CrysAlis RED*. Oxford Diffraction, England.
- Oxford Diffraction (2007a). *CrysAlis CCD*. Oxford Diffraction, Oxfordshire, England.
- Oxford Diffraction (2007b). *CrysAlis RED*. Oxford Diffraction, Oxfordshire, England.
- Plutecka, A., Hoffmann, M. & Rychlewska, U. (2007). *Struct. Chem.* **12**, 379–386.
- Sheldrick, G. M. (2008). *Acta Cryst.* **A64**, 112–122.
- Siemens (1990). *XP*. Siemens Analytical X-ray Instruments Inc., Madison, Wisconsin, USA.
- Spackman, M. A. & Jayatilaka, D. (2009). *CrystEngComm*, **11**, 19–32.
- Taylor, R. & Macrae, C. F. (2001). *Acta Cryst.* **B57**, 815–827.
- Wan, C.-Q., Chen, X.-D. & Mak, T. C. W. (2008). *CrystEngComm*, **10**, 475–478.
- Wolff, S. K., Grimwood, D. J., McKinnon, J. J., Jayatilaka, D. & Spackman, M. A. (2007). *CrystalExplorer2.1*. University of Western Australia.
- Yang, X., Wu, D., Ranford, J. D. & Vittal, J. J. (2005). *Cryst. Growth Des.* **5**, 41–43.